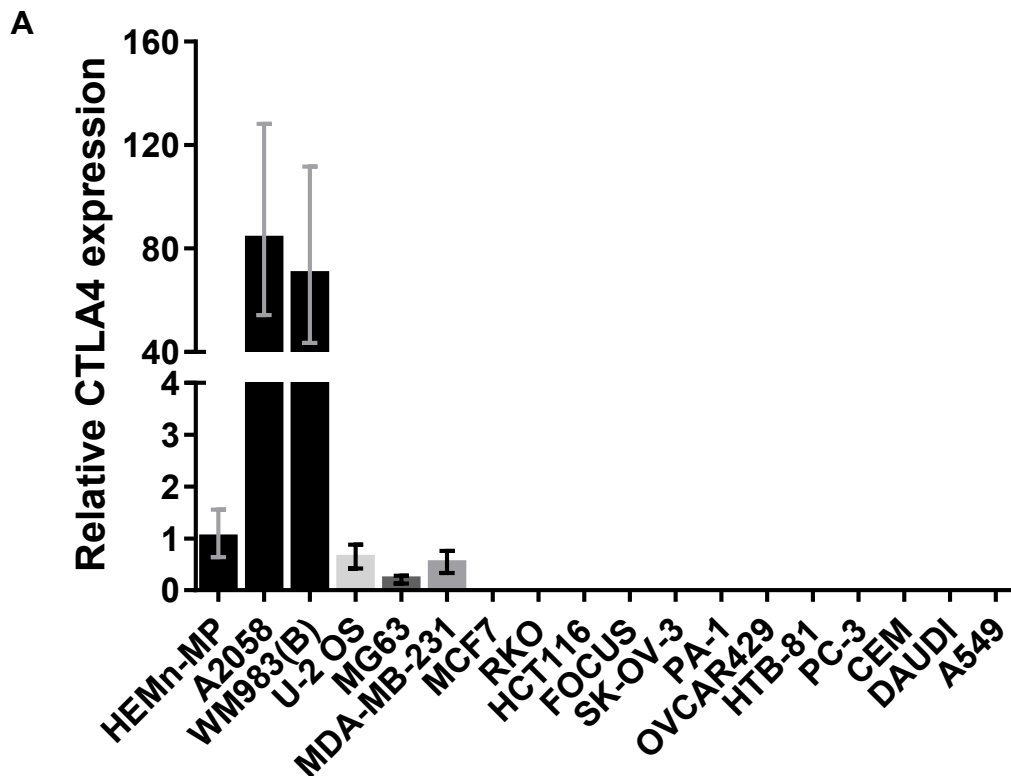


## Supplementary Figure S1

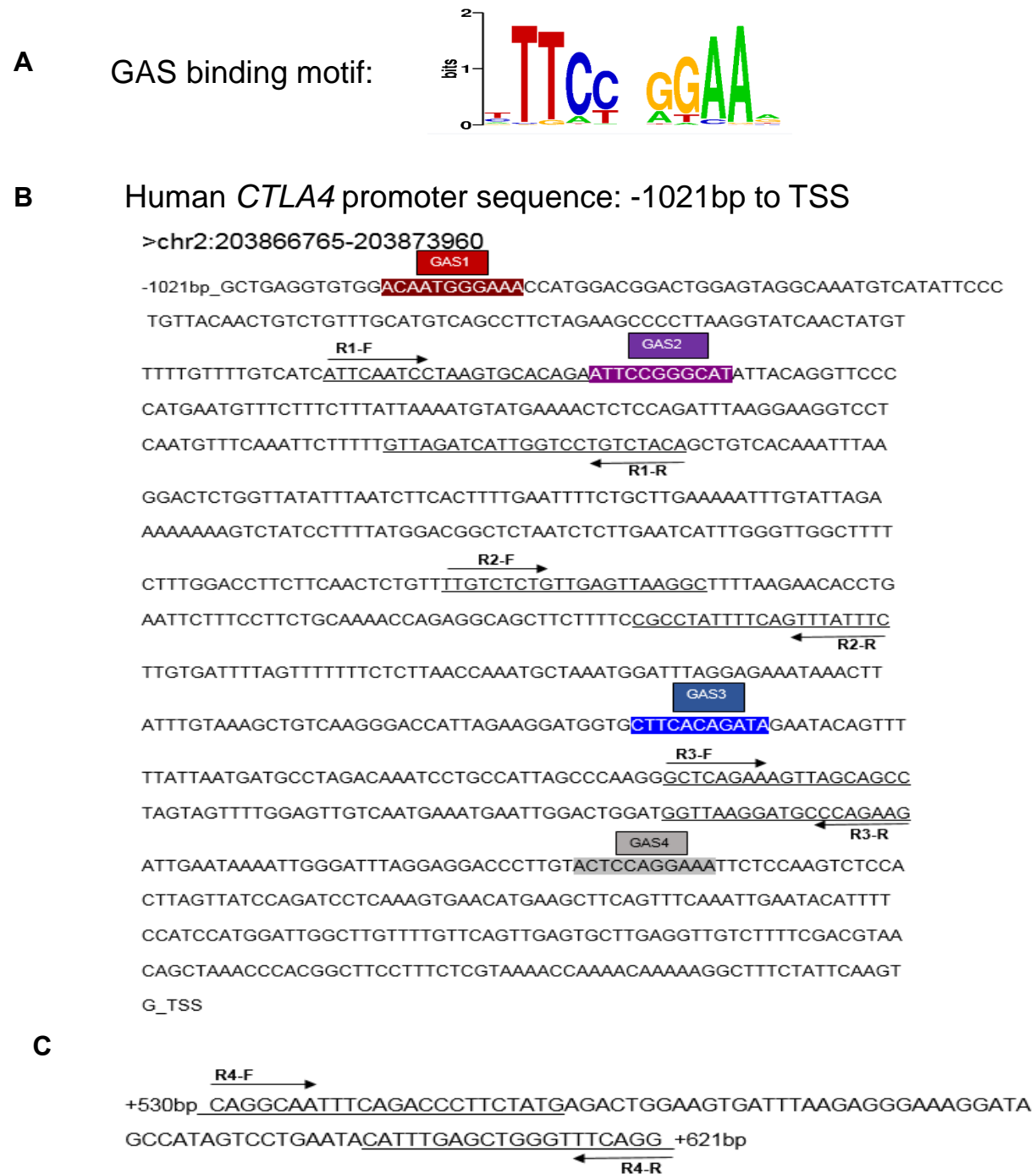


**B**

Cell line	Cancer types
U-2 OS; MG63	Human bone osteosarcoma
MDA-MB-231; MCF7	Human breast adenocarcinoma
RKO; HCT116	Human colon carcinoma
FOCUS	Human hepatocellular carcinoma
SK-OV-3; OVCAR429	Human ovarian adenocarcinoma
PA-1	Human ovarian teratocarcinoma
HTB-81; PC-3	Human prostate carcinoma
CEM	Human acute lymphoblastic leukemia
DAUDI	Burkitt's lymphoma
A549	Human lung carcinoma

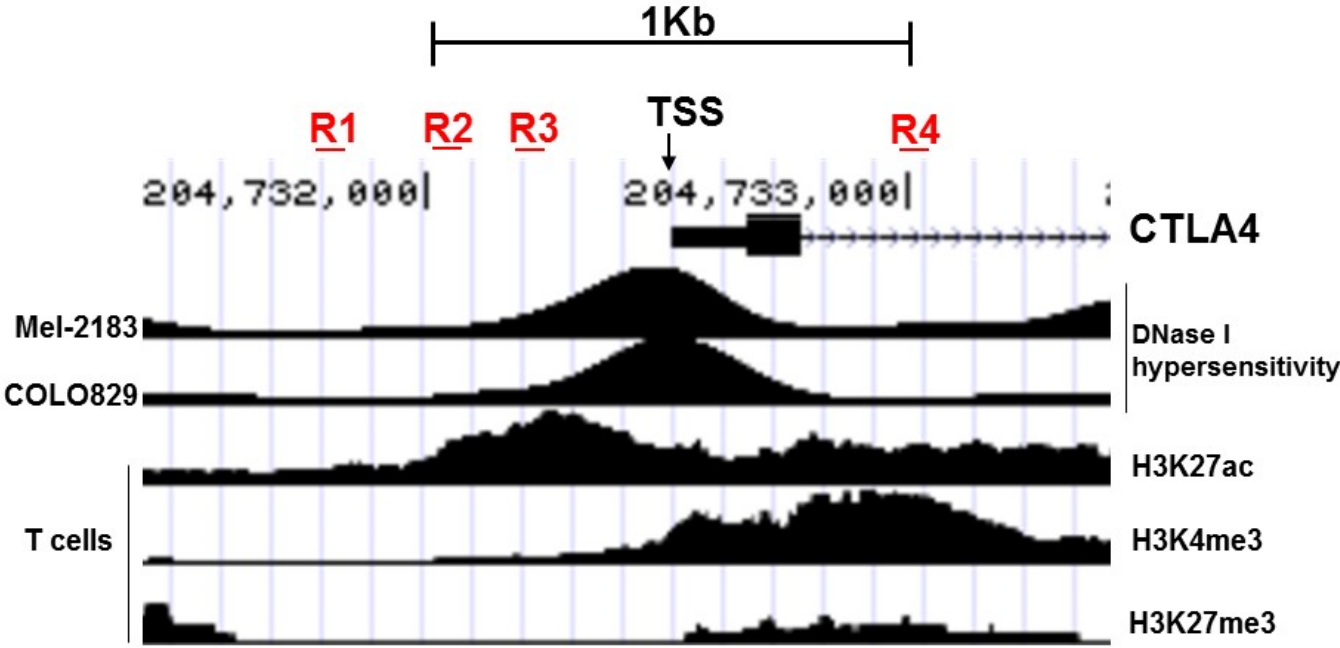
**Supplementary Fig. S1.** CTLA4 mRNA expression in human tumor cell lines. **A**, CTLA4 mRNA expression was determined by qRT-PCR, relative to HEMn-MP cells. Data are presented as mean $\pm$ SEM of three to six independent experiments. **B**, Types of cancer cell lines used in A.

## Supplementary Figure S2



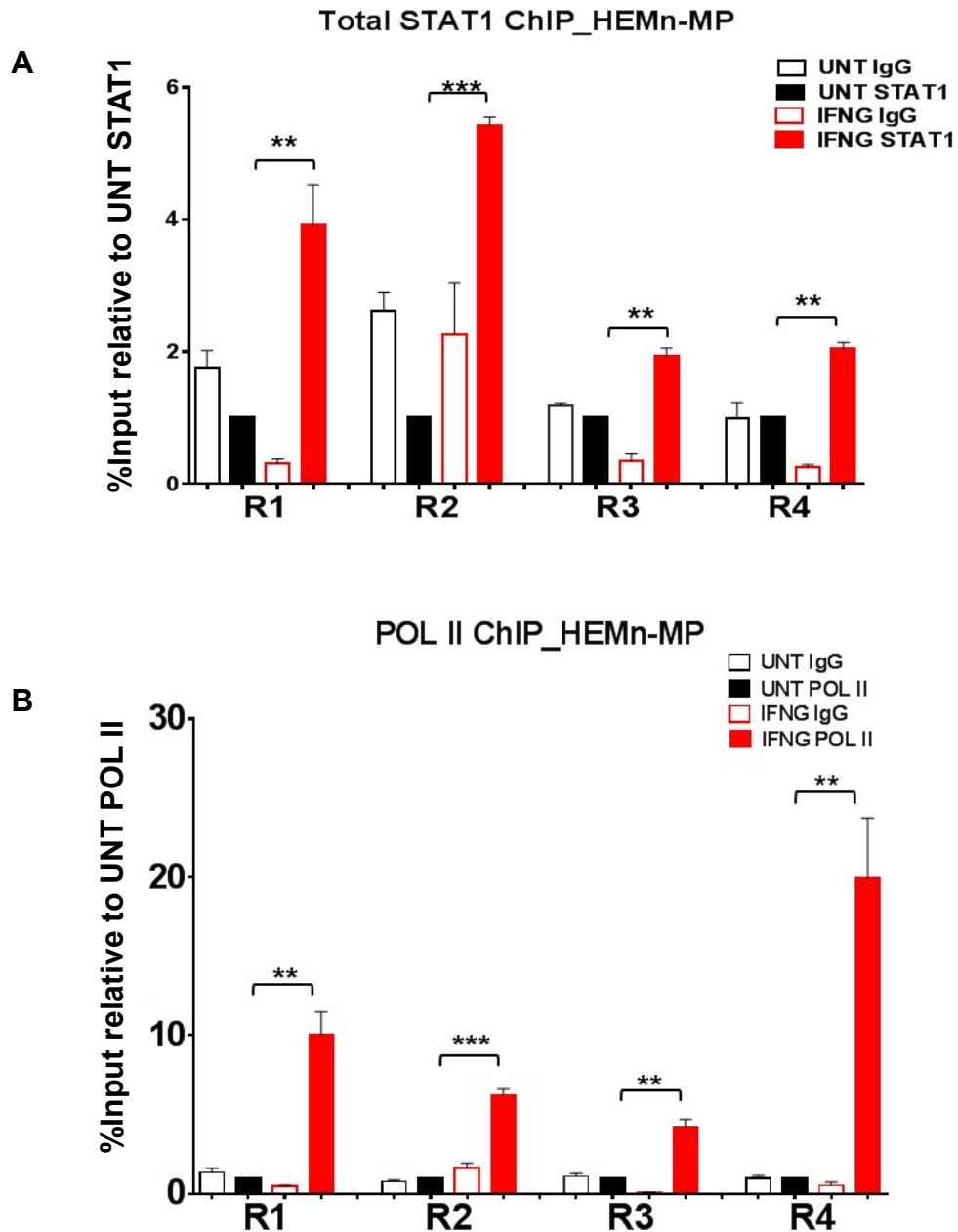
**Supplementary Fig. S2.** CTLA4 promoter analysis. **A**, Interferon-Gamma Activated Sequence (GAS) binding motif consensus sequence. **B**, Four putative GAS sites in human CTLA4 promoter sequence (-1021bp to TSS) are highlighted (GAS 1-4). Also shown are the primer sets used for detecting enrichment upstream of TSS by ChIP-qPCR assay in three different regions (R1-3). F, forward primer; R, reverse primer. **C**, Location of primer sets used for ChIP-qPCR assay for region downstream of TSS (R4).

# Supplementary Figure S3



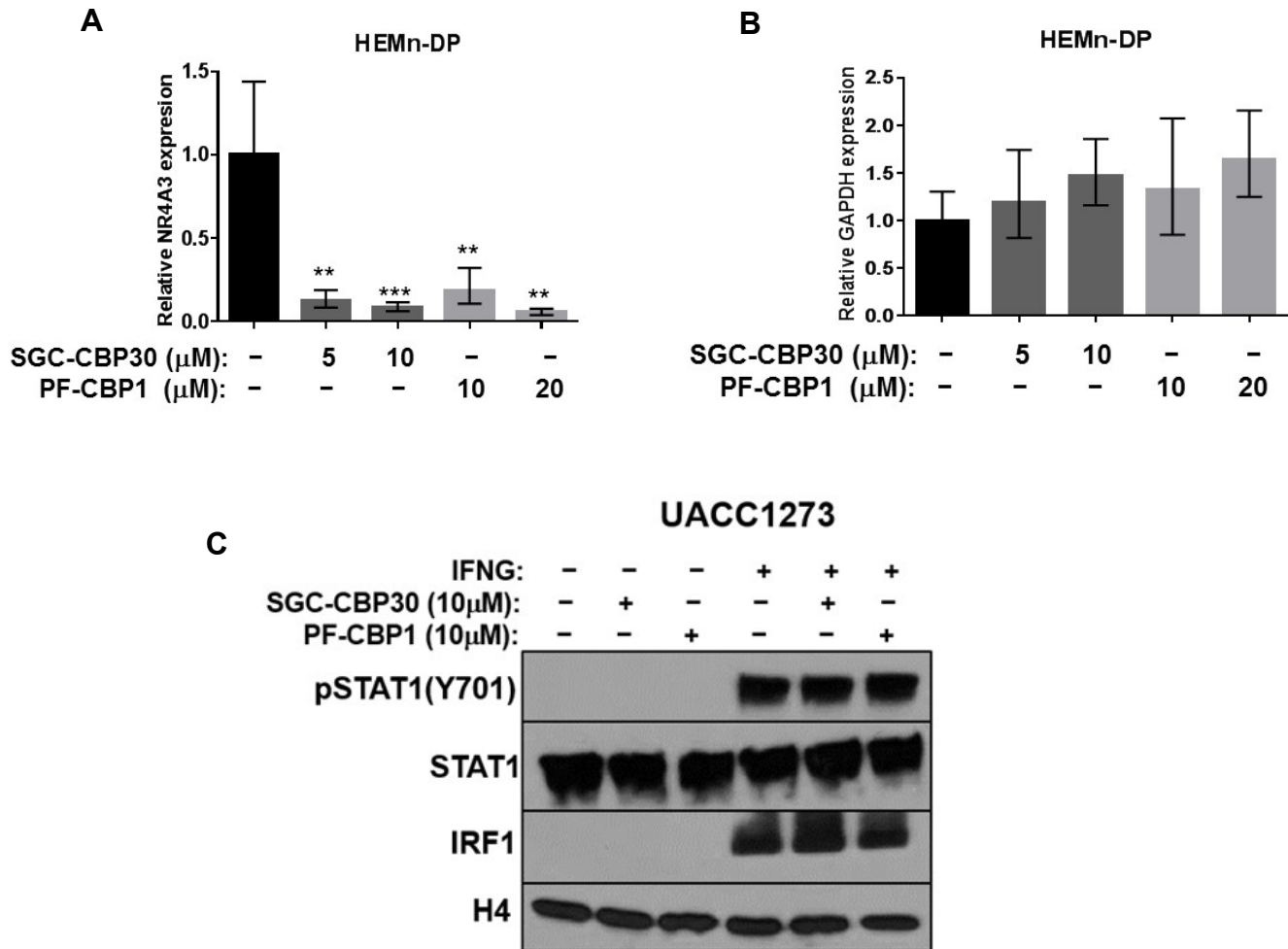
**Supplementary Fig. S3.** *CTLA4* promoter analysis. UCSC genome browser view shows the human *CTLA4* locus (GRCh37/hg19). DNase I hypersensitivity by DNase-seq analysis for human melanoma cell lines MEL-2183 and COLO829 and the ChIP-seq fold change signals over control for active promoter marks (H3K27ac, H3K4me3) and repressive mark H3K27me3 in human T cells were generated by ENCODE Project. The amplification regions R1 to R4 were used in ChIP-qPCR assay are indicated.

## Supplementary Figure S4



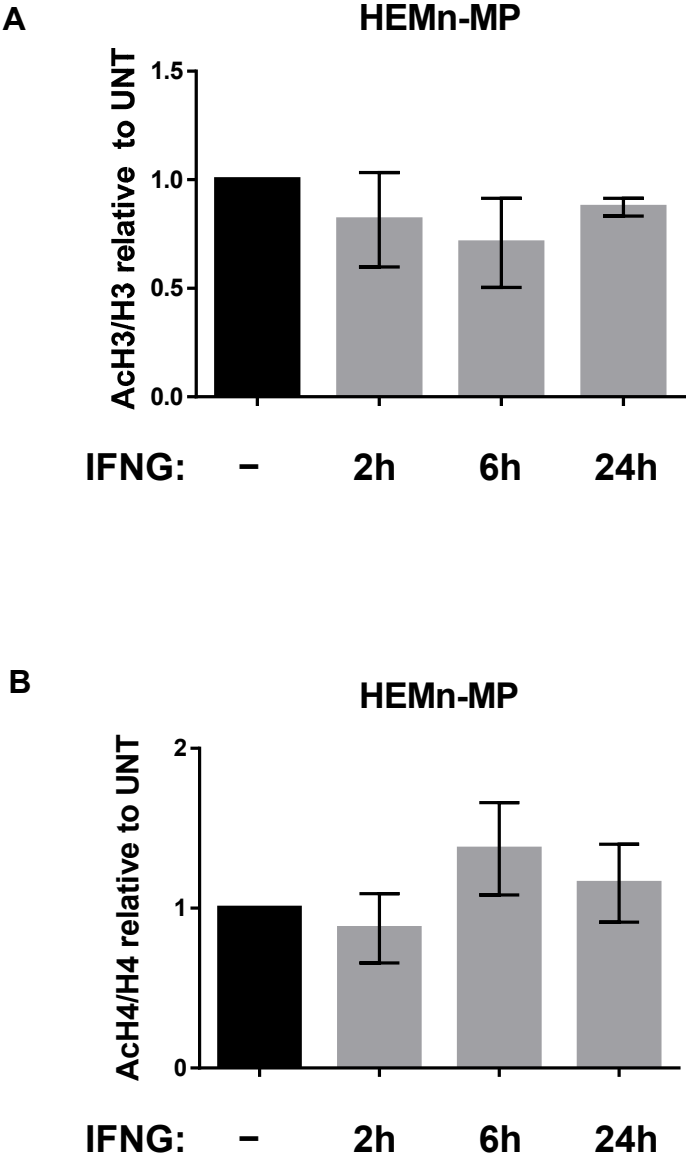
**Supplementary Fig. S4.** Recruitment of STAT1 and POL II to CTLA4 promoter by IFNG treatment. **A**, HEMn-MP cells were cultured in the presence or absence of IFNG for 7d before being subjected to chromatin immunoprecipitation (ChIP) and qRT-PCR assay with **(A)** anti-STAT1 antibody and **(B)** anti-POL II to measure recruitment to the *CTLA4* promoter. The sonicated nuclear extract before treatment with antibody were used as input. The relative abundance was calculated as %input and compared to the IFNG-UNT cells. \*\* $P < 0.01$ ; \*\*\* $P < 0.001$ .

## Supplementary Figure S5



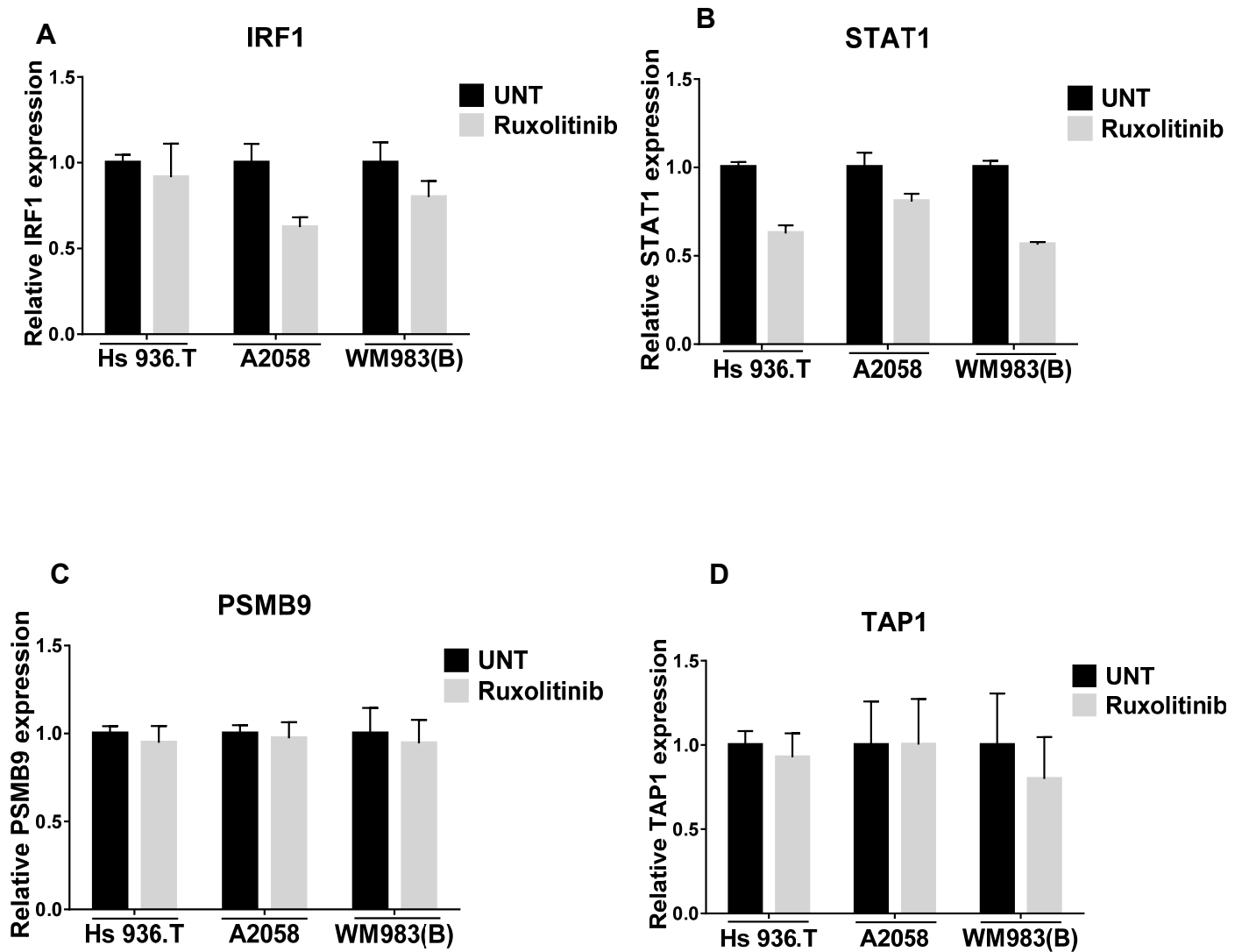
**Supplementary Fig. S5.** The effects of CBP inhibitors. **A**, qRT-PCR analysis showed that the CBP inhibitors SGC-CBP30 and PF-CBP1 inhibit expression of a known CBP target gene NR4A3 in HEMn-DP melanocytes after 1d of treatment, but **(B)** do not affect the expression of the housekeeping gene GAPDH. \*\*P < 0.01; \*\*\*P < 0.01. **C**, CBP inhibitor treatment does not affect IFNG signaling, as they failed to block phosphorylation of STAT1 and expression of IRF1 in response to IFNG treatment of UACC1273 melanoma cells. UACC1273 cells were pre-treated with either SGC-CBP30 (10uM) or PF-CBP1 (10uM) for 4h, then cultured in the presence or absence of IFNG for 4h before assessment of pSTAT1, total STAT1, and IRF1 expression levels by western blot. H4 was used as loading control.

# Supplementary Figure S6



**Supplementary Fig. S6.** Quantification of western blotting in **Fig. 5H** as mean±SEM of three independent experiments. Ratios of **A**, AcH3/H3 to untreated controls and **B**, AcH4/H4 to untreated controls.

## Supplementary Figure S7



**Supplementary Fig. S7.** The effects of Ruxolitinib on expression of genes of IFNG signaling pathway. Hs 936.T, A2058 and WM983(B) melanoma cells were treated with Ruxolitinib (5 $\mu$ M) for 24 hours and CTLA4 expression was measured by qRT-PCR analysis. **A**, IRF1, **B**, STAT1, **C**, PSMB9 and **D**, TAP1 expression after indicated treatments. Data are presented as mean $\pm$ SEM of three biological replicates. Ruxolitinib did not significantly affect the expression of these genes.